Authors Version of : Journal of Geophysical Research: Biogeosciences, vol.123(2); 2018; 463-478

Particulate organic carbon composition in temperature fronts of the northeastern Arabian Sea during winter

M.S Krishna[1], J. Mukherjee[1], H. B. Dalabehera[1], V.V.S.S. Sarma[1]
[1]CSIR-National Institute of Oceanography,
Regional Centre, Lawson's Bay colony,
Visakhapatnam, India
Corresponding author: Moturi Krishna (moturi@nio.org)

Abstract

In order to understand the major sources of particulate organic carbon (POC) in the frontal zones, and to examine their variability with space and time, a total of five temperature fronts of different ages were sampled in the northeastern Arabian Sea during winter. Compared to the non-frontal regions, POC and chlorophyll-*a* were higher within the coastal fronts whereas, chlorophyll-*a* was lower within the open ocean front (T1). The variation of POC between coastal and open ocean fronts is attributed to the combined influence of variable vertical mixing, heterotrophic transformation and age of the front. Relatively depleted $\delta^{13}C_{POC}$ and $\delta^{15}N_{PN}$ were observed within the fronts, suggesting that POC pool is contributed by *in-situ* production supported by upwelling of nutrient-rich water, and zooplankton biomass. Elemental C:N ratios, POC:Chl-*a*, $\delta^{13}C_{POC}$ and $\delta^{15}N_{PN}$ suggest that POC is mainly contributed from primary producers and heterotrophs in the study region. However, relative contributions from these two sources vary spatially from coastal to open ocean and with the age of the front. SIAR model revealed that zooplankton biomass largely contributed to POC in the open ocean (60-80%) than phytoplankton (20-40%) and nearly equal contribution was observed in the coastal fronts (50-60% and 40-50%, respectively). This study, thus, demonstrate that dominant heterotrophy and autotrophy in the open ocean and coastal fronts and it is consistent with their biomasses. Predominant heterotrophy in the open ocean is attributed to deeper mixed layer resulting in upwelling of bacteria-rich and phytoplankton-poor water to surface leading to existence of microbial loop.

Keywords: temperature fronts, nutrients, particulate organic carbon, Arabian Sea, primary production.

1. Introduction

Ocean fronts are commonly defined as the regions where the sharp horizontal gradient in physicochemical parameters, such as temperature, salinity, chlorophyll-*a*, occurs between two adjacent water masses [*Franks*, 1992; *Belkin and Commillon*, 2005; *Belkin et al.*, 2009]. Several mechanisms have been proposed for the formation of different types of fronts (upwelling, tidal, bouncy and topographic fronts) in estuarine, coastal and open ocean regions [*Franks*, 1992; *Asaro et al*., 2011; *Vipin et al*., 2015]. For instance, alongshore wind-stress at surface waters causes wind driven coastal fronts [*Halpern*, 1976; *Barton et al.*, 1977; *Shannon*, 1985], commonly known as the 'upwelling fronts'. More common mechanism for the formation of an oceanic temperature front is the upwelling of onshore flowing relatively cool deep water, which counterbalances the offshore Ekman flux of the surface waters, near the coast due to the upward bend and intersection of pycnocline with the surface [*Csanady*, 1982]. The main feature of the temperature front is the vertical mixing of relatively cool and nutrient-rich deep water with that of the surface [*Pollard and Regier*, 1990; *Rudnick and Luyten*, 1996; *Vipin et al.*, 2015]. Because of this vertical mixing, frontal regions are known to be biologically more productive [*Holligan et al.*, 1984a,b; *Dengler*, 1985; *Traganza et al.*, 1987; *Yoder et al.*, 1994; *Roy et al.*, 2015] and often sites of phytoplankton blooms [*Hesse et al.*, 1989; *Franks*, 1992; *Thurman and Trujillo*, 1999; *Levy et al.*, 2001; *Mahadevan and Tandon*, 2006; *Taylor and Ferrari*, 2011; *Olita et al.*, 2014; *Oguz et al.*, 2014]. Frontal instabilities that re-stratify the upper ocean further support primary production in the frontal regions. Even in the presence of surface winds and heat loss, the frontal instabilities are able to re-stratify the upper ocean [Fox-*Kemper et al.*, 2008; *Taylor and Ferrari*, 2010; *Thomas and Taylor*, 2010; *Mahadevan et al.*, 2010; *Taylor and Ferrari*, 2011] that inhibits vertical turbulent mixing and causes phytoplankton blooms. Relatively high phytoplankton biomass in the frontal zones attracts secondary producers that lead to fish aggregation [*Solanki et al.*, 2003; 2005]. Ocean fronts are generally developed at the edge of the filaments [*Ramp et al.*, 1991; *Haynes et al.*, 1993], with a high gradients in water properties. However, fronts may not be formed at the edges of all filaments [*Randerson and Simpson*, 1993] due to the diffusive boundaries rather than sharp gradients at the edge of some filaments.

Many studies were conducted on fronts and associated changes in the biogeochemical processes in the subtropical [*Mahadevan and Archer*, 2000; *Levy et al.*, 2001; *Mahadevan and Tandon*, 2006] and sub-polar regions [*Taylor and Ferrari*, 2011]. Such studies from the tropical regions, such as the north Indian Ocean, are very limited. The northeastern Arabian Sea (NEAS) is the only region, where the plenty of temperature fronts were reported [*Obenour*, 2014; *Vipin et al.*,

2015] during winter than any other region in the north Indian Ocean. The chlorophyll-rich fronts in the NEAS are shown to be linked to the shelf processes [*Vipin et al.*, 2015], as was observed elsewhere [*Strub et al.*, 1991; *Haynes et al.*, 1993; *Smyth et al.*, 2001], because they develop during bursts of cross-shore component of the west Indian coastal current (WICC) at the shelf break and advect offshore. *Amol et al.* [2014] reported that such current bursts occur frequently off the west coast of India during winter. Though, the temperature fronts are ubiquitous in the NEAS, during the winter monsoon [*Obenour*, 2014; *Vipin et al.*, 2015], however, the formation of temperature fronts and associated changes in the physical, chemical and biological processes remain poorly understood. Recently, some studies have focused on the front-induced changes in the biogeochemical processes in the NEAS.

Based on in-situ observations and satellite data, *Vipin et al.* [2015] suggested that pumping of water from the base of the ~60m thick mixed layer takes place within the frontal regions in the NEAS. In the same region, *Roy et al.* [2015] found relatively higher chlorophyll within the fronts compared to the surrounding waters and attributed it to the strong response of phytoplankton groups to the nutrient enrichment within the fronts. Relatively under-saturation of dissolved oxygen and higher dissolved inorganic carbon (DIC) were found within the fronts of the NEAS during winter [*Sarma et al.*, 2015]. The authors [*Sarma et al.*, 2015] suggested that the strength of the mixing process determines the front whether it is a source or sink of atmospheric CO_2. Very recently, it was also found that the depth integrated total bacterial count (TBC) and zooplankton biomass in the upper 50m of the water column were higher within the fronts than those outside the fronts in the NEAS [*Sarma et al.*, 2017]. All these studies were focussed on the vertical mixing of nutrients and associated changes in autotrophic and heterotrophic activities within the frontal regions. Although, the rapid cycling of carbon and nitrogen within the frontal zones decreases their turnover times compared to the surround non-frontal regions due to the active biological processes, such as high primary production, grazing pressure and microbial degradation in the former than the latter, however, the composition of particulate organic carbon (POC) and its cycling within the temperature fronts of the NEAS remain unclear. The main objectives of this study are to (i) examine variations in content of POC and PN in the frontal and non-frontal regions, (ii) evaluate variable sources of POC and PN in the frontal and non-frontal regions with reference to time (age of the front) and space (coastal and open ocean) and (iii) understand dominance of plankton (autotrophy or heterotrophy) in frontal regions of coastal and open ocean. Here, we present the results of five temperature fronts of different ages investigated in the coastal and open ocean regions of the NEAS during winter.

2. Study region

The Arabian Sea, the northwestern Indian Ocean, is one of the most productive zones in the world [*Madhupratap et al*., 1996; Smith, 2001; *Kumar et al.,* 2010] due to upwelling and convective mixing during southwest (SW) and northeast (NE) monsoons, respectively [*Shetye et al.,* 1994; *Madhupratap et al.,* 1996; *Muraleedharan and Prasannakumar*, 1996]. However, there exists a considerable spatial variability in the primary production over the basin, for example, the western Arabian Sea (off Somalia and off Oman) and the southeastern Arabian Sea (off southwest coast of India) are highly productive due to strong upwelling during SW monsoon [*Wyrtki,* 1971; *Unnikrishnan and Antony,* 1992; *McCreary et al.* 1996]. The present study region, the northeastern Arabian Sea (NEAS, off Saurashtra coast) is a productive zone during the NE monsoon (December – February) due to the winter convective mixing [*Banse and McClain,* 1986; *Prasannakumar and Prasad,* 1996; *Madhupratap et al.,* 1996]. The cool and dry winds blowing from the continents during this period [*Banse*, 1968; *Shetye*, 1998] causes evaporation leading to an increase in the sea surface salinity that deepens the mixed layer. Relatively deeper mixed layer, resulted from the convective mixing, brings nutrients into the euphotic zone and enhances the surface primary production in the NEAS during winter monsoon [*Banse,* 1984; *Madhupratap et al.,* 1996; *McCreary et al.,* 2009]. On the other hand, the deeper mixed layer than the depth of the euphotic zone during winter, however, tends to suppresses primary production in this region, despite nutrients are available [*Naqvi et al.,* 2002].

2.1. Temperature fronts in the NEAS

The offshore Ekman flux of surface waters during winter, due to the equatorward flowing wind stress in eastern ocean basin of the north-south oriented coast (west coast of India), is counter balanced by the flow of deep water in the onshore direction which upwells to the surface near the coast, generating temperature fronts during this period. The occurrence of these meso-scale features enhances the surface primary production in NEAS during winter monsoon [*Roy et al.,* 2015] by injection of nutrients into the euphotic zone through vertical mixing from base of the mixed layer [*Vipin et al.,* 2015]. Though, the horizontal temperature gradients are weaker in the tropics (2-5^{o}C) [*Lendt et al.,* 1999; *Barber et al.,* 2001] than the sub-tropical and temperate regions (10-15^{o}C) [*Dong et al.,* 2006; *Belkin et al.,* 2009], however, the weak upwelling velocities are quite enough to pump water into the surface from the base of the mixed layer in the NEAS [*Vipin et al.,* 2015]. The fronts move along with currents in the northwestward direction due to prevailing currents during winter monsoon last for few days, typically 1-2 weeks. The temperature fronts in the NEAS extend from 10 to 20 km in width and about 100 km in length [*Vipin et al.,* 2015]. In the present study, the fronts of

different ages at the time of their sampling, ranging from as young as 0.5 to as old as 11 days [*Sarma et al.,* 2017], in the NEAS were investigated. Among the five fronts sampled, front T5 is the youngest (0.5 day) following T1 (3.3 days), T2 (6 days), whereas T3 and T4 are the oldest (9-11 days) at the time of our sampling [*Sarma et al.,* 2017]

3. Material and Methods

3.1 Sample collection

A cruise onboard research vessel Sindhu Sankalp (#SSK-60) was undertaken from 22nd January to 3rd February, 2014 for in-situ observations and sampling in the frontal and surrounding non-frontal (NF) regions of the northeastern Arabian Sea (Fig. 1). A total of five fronts were sampled in the NEAS; two fronts in the open ocean (fronts T1 and T2), two fronts in the coastal region (T4 and T5), and one in between (T3) (Fig. 1). Water samples at different depth intervals were taken by using a Conductivity-Temperature-Depth (CTD) profiler attached to the rosette system (Seabird, USA) fitted with 10 L Niskin bottles. Water samples (4.5 ml) in triplicate were fixed with 1% paraformaldehyde (final concentration) and stored at -80^{o}C until analysis of total bacterial count (TBC) in the onshore laboratory. Zooplankton samples were collected by vertical hauling of 200 µm cylindrical net along with CTD-rosette system from 50m below surface to the surface. Meso-zooplankton samples were collected through 200µm bongo net while phytoplankton samples were obtained by passing the seawater sample through 10µm mesh.

3.2 Biogeochemical parameters

High resolution temperature and salinity data was obtained from CTD (SBE 19 plus) attached to the rosette. Dissolved inorganic nutrients (nitrate, nitrite, phosphate and silicate) were determined by the colorimetric procedure using an Autoanalyzer (Skalar San Plus, The Netherlands) following [*Grashoff et al.,* 1992]. Dissolved oxygen (DO) concentrations were measured by the Winkler titration method [*Carritt and Carpenter*, 1966] using a potentiometric end point detection (Titrando 835; Metrohm, Switzerland). Water samples (~5L) were filtered through a pre-combusted (300^{o}C; 6 hours) GF/F filters (nominal pore size: 0.7 µm; 47 mm diameter; Whatman) at a moderate vacuum and the filtrate was stored at -20^{o}C until further analysis of content and stable isotopes of carbon (C) and nitrogen (N). The phytoplankton biomass (Chlorophyll-*a*) on the filtrate obtained by filtering ~5L of seawater through GF/F filter under moderate vacuum was determined using high pressure liquid chromatography (Agilent 1200, USA) following *Van Heukelem* [2002]. The detailed procedure was described elsewhere [*Roy et al.,* 2006; 2015]. Since the zooplankton samples were collected by vertical hauling from 50m deep to surface, the estimated zooplankton biomass reported

here is an integrated value in the upper 50m of the water column in all stations. For TBC analysis, the frozen samples were thawed to room temperature and stained with SYBR Green I (1:10000, Molecular probes, USA) and kept for incubation in the dark. After completion of incubation period of 15 minutes, flow cytometric absolute cell counting was done using BD FACS Aria II instrument fitted with 488 nm blue laser with sheath fluid of BD FACS flow. The filter sets 488/10 and 530/30 band passes collected the emitted light for right angle light scatter and green fluorescence, respectively. Fluorescent beads of 1 μm (Polysciences) were used as internal standards and for calibration [*Khandeparker et al.,* 2017]. The software BD FACS ARIA II was used to process the flow cytometric data. Nutrients, DO, Zooplankton biomass and TBC data of these fronts were described in detail elsewhere [*Sarma et al.,* 2017].

The age of a front, at the time of sampling, was determined by tracking its evolution and movement using sea surface temperature (SST) images from MeTop-B, NOAA-18, and NOAA-19 continuously for 10-15 days, with a temporal resolution of six times in a day, based the availability of a cloud-free SST images. The time elapsed between its evolution and sampling was taken as the age of the front. Variations in the shape and size of the fronts with time after its evolution were also considered for determining the age of a front.

3.3 Content and stable isotopes of POC and particulate nitrogen (PN)

The GF/F filters stored at -20^{o}C brought to room temperature and dried in an oven for 24 hours at 60^{o}C. An aliquot of the filter was acid fumigated for 12h in a desiccator to remove the traces of inorganic carbon. The content of POC and PN on the filter, and their stable isotope ratios ($\delta^{13}C_{POC}$ and $\delta^{15}N_{PN}$, respectively) were measured using an elemental analyzer (Flash EA, Thermo Electron, Germany) coupled to an isotope ratios mass spectrophotometer (Delta V plus, Thermo) via conflo IV interface. Internal reference materials, such as Glutamic Acid, Alanine, Marine sediments and IAEA standards were used for internal calibration. The long term precision of the instrument was ±0.02% for content and ±0.2‰ for stable isotope ratios of both carbon and nitrogen [*Sarma et al.,* 2012; 2014]. The results of $\delta^{13}C_{POC}$ and $\delta^{15}N_{PN}$ were expressed in δ notation as given below.

$$\delta R = \left[\frac{X_{samp}}{X_{std}} - 1\right] x\ 10^3\ ‰$$

where R = ^{13}C or ^{15}N, X_{std} = $^{13}C/^{12}C$ or $^{15}N/^{14}N$ of standard and X_{sam} = $^{13}C/^{12}C$ or $^{15}N/^{14}N$ of sample for carbon and nitrogen respectively.

3.4 δ^{13}C and δ^{15}N of phytoplankton and meso-zooplankton

Specimens of meso-zooplankton and phytoplankton (group level) were identified under the microscope and picked out into tin cups using an injection syringe and needle. The tin cups along with specimens were dried at 60°C for 12h. The content and isotopic ratios of C and N in the dried samples were measured using an elemental analyzer coupled to Isotope ratio mass spectrometer (EA-IRMS-Delta V, Finnigan, Germany) through Conflo IV interface, and the results were expressed in δ notation as mentioned above.

3.5 Estimation of proportional contributions of organic matter from major sources

Dual isotope mixing model SIAR (Stable Isotope Analysis in R) that solves mixing models within a Bayesian framework [*Parnell et al.* 2008; 2010] was used to estimate the proportional contributions from major sources to the POC pool within the fronts. The advantage of this model is that the inclusion of the residual error term in the form of standard deviation, unlike the model MixSIR [*Jackson et al.*, 2009; *Parnell et al.*, 2010]. Complete description of the model was given elsewhere [*Krishna et al.*, 2014]. The model 'SIAR' has been used for the source apportionment of organic matter in the coastal regions elsewhere [*Dubois et al.*, 2012; *Carreon-Palau et al.,* 2013; *Krishna et al.,* 2014; *Sarma et al.,* 2014). However, the selection of the end members is critical for the estimation of proportional contributions from different sources. The measured $\delta^{13}C$ and $\delta^{15}N$ of phytoplankton and zooplankton groups collected from the frontal regions of the present study were used as end members in the model. Software program 'Ocean Data View' (ODV; version 4.0) was used for graphical representation of the data and VG gridding was used for extrapolation.

4. Results

SST ranged from 23.8 to 24.8^{o}C in the frontal and from 24.9 to 25.4^{o}C in the non-frontal regions. Mean temperature difference in the upper 50m of the water column between within and outside the fronts varied from as low as 0.4^{o}C (in front T1) to as high as 1.6^{o}C (in front T2). Fronts, T3 (0.6 ^{o}C), T4 (0.6 ^{o}C) and T5 (0.5 ^{o}C) showed intermediate values (Fig. 2; Table 1).

4.1 Phytoplankton and zooplankton biomass in the frontal and non-frontal regions

Phytoplankton biomass, in terms of Chlorophyll-*a* (Chl-*a*), showed considerable difference between the frontal and non-frontal regions of the open (T1 and T2) and coastal (T3, T4 and T5) oceans. Integrated Chl-*a* in the upper 50m of the water column was relatively higher within the coastal fronts T3 (36.2 mg m^{-2}), T4 (27.4) and T5 (44.1 mg m^{-2}) and open ocean front T2 (67.9 mg m^{-2}) than their non-frontal regions (27.8, 23.2, 18.2 and 31.6 mg m^{-2}, respectively) (Table 1). In contrast, Chl-*a* was slightly lower within the open ocean front T1 (30.1 mg m^{-2}) than the surrounding non-frontal region (31.5 mg m^{-2}) (Table 1). All the fronts, T1, T2, T3, T4 and T5, recorded

relatively higher zooplankton biomass within the fronts (576, 906, 1919, 3379 and 1649 mg m^{-2}, respectively) than those observed outside region of these fronts (177, 480, 1154, 1258 and 1137 mg m^{-2}, respectively). Relatively higher TBC was found within the open ocean fronts T1 and T2 ($1.30x10^8$ and $4.12x10^8$ Nos. l^{-1}, respectively) than the non-frontal regions ($0.70x10^8$ and $1.17x10^8$ Nos. l^{-1}), whereas, more or less similar TBC was found within the front and non-frontal regions of T4 ($0.90x10^8$ and $0.85x10^8$ Nos. l^{-1}, respectively) and T5 ($1.33x10^8$ and $1.30x10^8$ Nos. l^{-1}). However, relatively lower TBC was found in the frontal ($1.04x10^8$ Nos. l^{-1}) than non-frontal region ($1.28x10^8$ Nos. l^{-1}) of T3.

4.2 Content of POC and PN in the frontal and non-frontal regions

Mean POC concentrations in the surface were relatively lower within the open ocean fronts T1 (114 µg L^{-1}) and T2 (179 µg L^{-1}) than those outside the fronts (193 and 210 µg L^{-1}, respectively) (Fig. 2). Integrated POC content in the upper 50m of the water column was higher within the front (5352 µg m^{-2}) than outside the front T1 (4704 µg m^{-2}). However, the difference is negligible in the front T2 (5253 and 5159 µg m^{-2}, respectively) (Table 1). Relatively lower POC and PN was observed in the coastal front T4 (5144 and 25.2 mg m^{-2}, respectively) than the non-frontal region (5916 and 30.8 mg m^{-2} respectively). Similar concentration of POC was found in the frontal and non-frontal regions of T2 (5159 and 5253 mg m^{-2}, respectively) and T3 (4623 and 4729 mg m^{-2}, respectively).

Integrated PN content in the upper 50m of the water column was higher in the non-front T2 (1190 µg m^{-2}) than within the front (1014 µg m^{-2}), whereas this difference is small in the front T1 (957 and 940 µg m^{-2}, respectively) (Table 1). Coastal fronts showed a contrasting pattern to that of the open ocean fronts, with a relatively higher integrated POC within the fronts T3 (mean 4778 µg m^{-2}), T4 (5306) and T5 (6591) compared to those of the non-frontal regions of these fronts (4219, 5027 and 6144 µg m^{-2}, respectively; Table 1). Similarly, integrated PN was also higher within the coastal fronts T3 (1367 µg m^{-2}), T4 (1354) and T5 (1323 µg m^{-2}) than non-frontal region of these fronts (1230, 1313, and 1222 µg m^{-2} respectively, Table 1), consistent with that of the POC distribution. Mean elemental C:N ratios in the upper 50m of the water column ranged from 4.8 to 8.0, with a relatively higher ratios within the frontal regions of the open ocean (mean: 6.9±2.8) than the coastal ocean (5.0±2.0) (Fig. 3).

4.3 Stable isotopes of POC ($\delta^{13}C_{POC}$) and PN ($\delta^{15}N_{PN}$) in the frontal and non-frontal regions

The $\delta^{13}C_{POC}$ in the surface ranged from -26.3 to -24.4‰ in the frontal and from -26.1 to -23.5‰ (Table 2) in the non-frontal regions. Slightly depleted $\delta^{13}C_{POC}$ were observed within the fronts T1 (-25.2‰), T2 (-26.1) and T5 (-25.7) than the surrounding non-frontal regions (-24.5, -25.5 and -

24.4‰, respectively, Table 2). The mean $\delta^{13}C_{POC}$ were relatively depleted within the fronts (-25.7±0.4‰) than the non-frontal regions (-24.8±0.6‰), except for the fronts T3 and T4 where relatively enriched $\delta^{13}C_{POC}$ were observed within the fronts (-24.6 and -25.3‰, respectively) than the non-frontal regions (-25.1 and -25.7‰). The $\delta^{15}N_{PN}$ in the surface varied from 4.7 to 13.7‰ and from 5.2 to 26.6‰, in the frontal and non-frontal regions, respectively (Table 2). Relatively depleted $\delta^{15}N_{PN}$ were observed within the fronts (8.4±1.7‰) than the surrounding non-frontal regions (12.8±5.7), except the front T4, where $\delta^{15}N_{PN}$ was slightly enriched within (10.5‰) than outside (10.0‰) front.

In order to understand the statistical significance of the difference between frontal and non-frontal regions of several variables, a homoscedastic (two-sample equal variance) Student's t-Test with a two tailed distribution was performed between the frontal and non-frontal regions. The probability (p) associated with this t-test for different variables were listed in Table 3. Except $\delta^{15}N_{PN}$ in fronts T4 and T5, the remaining variables showed statistically significant difference between the frontal and non-frontal regions (Table 3).

4.4. Isotopic composition of phytoplankton and zooplankton in the frontal and non-frontal regions

The $\delta^{13}C$ of dominant phytoplankton groups collected in the study region (diatoms and dinoflagellates) showed slightly depleted values within the fronts (-25.1±0.5‰) than the non-frontal regions (-24.2±0.7‰, Table 2). Similarly, zooplankton also showed relatively depleted $\delta^{13}C$ within the fronts (-25.4±0.6‰) compared to those observed in the non-frontal region (-24.6±0.1‰, Table 2). On the other hand, both phytoplankton and zooplankton were characterized by the relatively enriched $\delta^{15}N$ in the frontal (4.2±0.3 and 5.8±0.5‰, respectively) than the non-frontal regions (3.8±0.3 and 5.0±0.5‰, respectively) (Table 2), contrasting to that of the $\delta^{13}C$.

5. Discussion

5.1 Variable hydrographic conditions and sources of nutrients in temperature fronts

The SST difference between the frontal and non-frontal regions of this study are similar to those observed earlier in the northeastern Arabian Sea (0.3-1.0^{o}C) [*Vipin et al.,* 2015; *Roy et al.,* 2015, *Sarma et al.,* 2015] and the western Arabian Sea [*Lendt et al.,* 1999; *Barber et al.,* 2001], but weaker than those reported elsewhere in the world oceans [*Hickox et al.,* 2000], for example, Florida Current (2-10^{o}C) and the Gulf Steam (1.5-4.5^{o}C) [*Belkin et al.,* 2009] and in the temperate region [*Moore et al.,* 1999; *Dong et al.,* 2006] due to variable mixing rates [*Park and Chu,* 2006].

Prevailing hydrographic conditions in the frontal and non-frontal regions of the temperature fronts (T1 to T5) in the NEAS during the study period were given in detail elsewhere [*Sarma et al.,*

2017]. Briefly, the distribution of temperature and salinity in the upper 50 m of the water column (Fig. 2) showed an upwelling of the high salinity and cooler deep waters into the surface within the frontal regions. An inverse relationship between nutrients and temperature indicates an upwelling of nutrient-rich sub-surface waters in to the surface within the fronts, resulting in relatively higher concentrations of integrated nutrients in the mixed layer of the frontal regions compared to the surrounding non-frontal regions. A significant linear relationship between nutrients and the depth-integrated phytoplankton biomass indicated that the nutrients injected into mixed layer through the upwelling supported the primary production within the frontal regions. As a result, relatively higher integrated phytoplankton biomass was found within the frontal than the corresponding non-frontal regions, except T1 (Table 1). Further, phytoplankton cells were found to be healthy and active within the frontal than the non-frontal regions from relatively higher Fv/Fm ratios in the former than the latter [*Sarma et al.*, 2017].

Although, the fronts were identified by the difference in SST at the time of our sampling, however, characterization of the frontal and non-frontal region is a difficult task because the front is dynamic in nature and laterally advects in the direction of the mean flow. Since, the prevailing currents in the NEAS during our study period were in the northwestward, the fronts move laterally towards northwest direction [*Sarma et al.*, 2017]. The open ocean fronts T1 and T2 were sampled from northwest to southeast direction, while the coastal fronts T3 and T5 were sampled from east to west except T4 which was sampled from west to east (Fig. 1). Therefore, non-frontal regions in our study might have influenced by the fronts before our sampling. Further, some residual signatures were found to be left behind after the movement of the front. For instance, *Vipin et al.* [2015] noticed residual chlorophyll signals after the front had passed the region. Nevertheless, the prevailing conditions in the surrounding non-frontal region at the time of our sampling were considered as initial (background) conditions because the upwelling of subsurface waters with different characteristics changes the initial surface conditions within the fronts. The background conditions from which fronts evolve are important in understanding the variability of particulate organic matter (POM) within the frontal regions of coastal and open oceans.

5.2 Variations in the content of POC and PN in the frontal and non-frontal regions

The range of POC concentrations observed in this study is similar to those reported earlier in the eastern Arabian Sea [*Sardessai et al.*, 1999]. Relatively higher POC within the frontal than the non-frontal region (Table 1 and 3) can be explained by the enhanced primary production in the former than the latter as relatively higher integrated Chl-*a* was found within the frontal (mean 41±16 mg m^{-2}) than the non-frontal regions (26±6 mg m^{-2}). A significant linear relationship between the

integrated POC and phytoplankton biomass (Chl-*a*) (r^2=0.48; p<0.001) conform that significant contribution of organic matter from in-situ production during the study period. Elevated primary production within the frontal regions could be due to (i) the availability of nutrients that were brought to the surface by upwelling of the nutrient-rich subsurface water into the surface [*Levy*, 2001; *Mahadevan et al.*, 2008; *Vipin et al.*, 2015] and (ii) re-stratification of the water column by the frontal instabilities [*Fox-Kemper et al.*, 2008; *Mahadevan et al.*, 2010; *Thomas and Taylor*, 2010; *Behrenfeld*, 2010; *Taylor and Ferrari*, 2010] which hinders the turbulent vertical mixing in the frontal zones. A negative relationship of nitrate with Chl-*a* within the frontal regions (r^2=0.30; p<0.001) suggests nutrients injected into euphotic one by vertical mixing supported *in-situ* primary production in the frontal regions. Elevated levels of primary production within the ocean fronts was also reported in the NEAS [*Roy et al.*, 2015; *Sarma et al.*, 2015; 2017] and elsewhere in the world oceans [*Mahadevan and Archer*, 2000; *Levy et al.*, 2001; *Mahadevan and Tandon*, 2006; *Taylor and Ferrari*, 2011; *Olita et al.*, 2014], and attributed to the input of nutrients in to euphotic zone through the upwelling/vertical mixing.

However, POC was higher in the frontal than the non-frontal region of T1 (Student t-test, p=0.63; Table 3) despite Chl-*a* was similar in the former and latter regions (Table 1). On the other hand, POC concentrations were nearly equal in the frontal and non-frontal regions, despite Chl-*a* was significantly higher in the former than the latter regions of T2 and T3 (Table 1). The decoupling between Chl-*a* and POC and a weak negative relationship between nitrate and POC (r^2=0.31, p<0.001) in the frontal regions suggests dominant contribution from heterotrophs, or conversion of POC to dissolved organic carbon (DOC) and/or initial background conditions. Relatively higher zooplankton biomass and TBC (except T3) were observed in the frontal regions than the corresponding non-frontal regions (Table 1), suggesting that significant contribution from heterotrophs may be possible within the fronts than the non-frontal regions. Significant negative relationship between zooplankton biomass and POC (r^2= -0.41; p<0.001) suggests that zooplankton may be feeding on POC. A linear relationship of TBC with pCO_2 (r^2=0.43; p<0.001) and an inverse relation with the dissolved oxygen (r^2=-0.45; p<0.001) within fronts of this region [*Sarma et al.*, 2015, 2017] indicate an intense bacterial decomposition of organic matter within the fronts compared to the surrounding non-frontal regions lead to conversion of POC to DOC is possible. However, no DOC data are available to compare.

Three times higher zooplankton biomass in the coastal fronts (mean of T3, T4 and T5: 2316±930 mg m^{-2}) than that of the open ocean fronts (mean of T1 and T2: 741±233 mg m^{-2}), and less than half of the TBC in the former (1.09±0.2 No. l^{-1}) compared to that of the latter (2.71±2.0 No. l^{-1})

suggest that dominant heterotrophic activity by zooplankton in the coastal and by bacteria in the open ocean fronts. Dominance of microbial activity in the open ocean fronts could be due to the predominant contribution from *Phaeocystis* (*Prymnesiophyte*) to the phytoplankton biomass within the fronts of the open ocean region of the NEAS during winter [*Roy et al.,* 2015]. This is because *Phaeocystis* are known for production of higher DOC and therefore support microbial carbon demand [*Smith et al.,* 1998] within the frontal regions. Further, the grazing activity of *Phaeocystis* blooms was found to be higher but species dependent [*Schoemann et al.,* 2005]. Relatively higher concentrations of 19′ hexanoyloxyfucoxanthin, 19′-butynoyloxyfucoxanthin and fucoxanthin, the marker pigments for *Prymnesiophytes,* within the open ocean fronts of the present study [*Dr. R. Roy, personal communication*] confirms that significant contribution from *Phaeocystis* to the phytoplankton biomass. Phytoplankton composition is, therefore, responsible, at least partly, for variable contributions to POC from different heterotrophs. However, the difference in biological response between coastal and open ocean fronts may also be due to variable mixing depth of the front and initial conditions. Deeper mixed layer in the open ocean (63±6m) than the coastal ocean fronts (38±8m) brought the TBC-rich subsurface waters to the surface in the former that might have led to existence of microbial loop in the former and dominance of heterotrophic activity than autotrophic. In contrast, shallow mixed layer in the coastal fronts results in the upwelling of nutrient rich and subsurface Chl-*a* to the surface leading to dominance of autotrophy than heterotrophy. Nevertheless, the variability of POC within the frontal regions of coastal and open ocean could be due to the balance between autotrophic production and heterotrophic consumption. This balance may vary with the age of the front and initial background conditions due to variable response of ecosystem components to nutrient enrichment.

The younger fronts T5 (0.5 days) and T1 (3.3 days) showed higher POC in frontal regions (6591 and 5352 mg m^{-2}, respectively) than the non-frontal region (6144 and 4704 mg m^{-2}, respectively) (Table 3), whereas the relatively older fronts T2 (6 days), T3 (9 days) and T4 (11 days) showed lower POC within the frontal (5159, 4623 and 5144 mg m^{-2}, respectively) than the respective non-frontal regions (5253, 4729 and 5916 mg m^{-2}, respectively) (Table 3). This suggests that production dominates over consumption (autotrophy) when fronts are formed and the dominance shifts towards heterotrophy with increasing the age of the front due to the lag in heterotrophs to respond to autotrophic production. Although, the open ocean front T1 is the youngest among the fronts sampled in this study, however, relatively higher TBC within the frontal ($1.30x10^8$ Nos. l^{-1}) than the non-frontal ($0.70x10^8$ Nos. l^{-1}) region is due to the mixing of TBC-rich deeper waters with that of the surface because TBC was higher at depth (~50-60m) in this region [*Sarma et al.,* 2017]

and mixing depths are deeper (63±6m) in the open ocean. Hence, the higher TBC may not probably be due to the age-related shifting from autotrophy to heterotrophy.

No studies on POC or its stable C isotopes are available, to the best of our knowledge, in the frontal regions of either the Arabian Sea or the Bay of Bengal to compare our results. However, our findings of higher POC and intense autotrophic and heterotrophic activities within the frontal regions are concurrent with earlier reports on frontal regions elsewhere [*see review by Owen,* 1981], for instance, northwest off Cape Town, South Africa [*Bang,* 1973], Sargasso Sea [*Hulbert,* 1964; Colton et al., 1975]; Cape Columbine upwelling centre in the Southern Benguela [*Armstrong et al.,* 1987] and California Current off Southern California [*Li et al.,* 2012; *Ohman et al.,* 2012; *Stukel et al.,* 2017].

5.3. Potential sources of POC in the frontal region

The range of elemental C:N ratios observed within the upper 50m of the open ocean (mean 6.3±2.0) and coastal (5.5±1.9) fronts are close to the C:N ratios of phytoplankton derived organic matter (6-8) [*Redfield et al.,* 1963; *Onstad et al.,* 2000; *Jennerjahn et al.,* 2004], but slightly higher than the bacterial biomass (3-6) [*Le Fevre-Lehoerff et al.,* 1993, *Creach,* 1995; *Hedges et al.,* 1997] and zooplankton biomass (3-6) [*Koski,* 1999; *Fagerbakke et al.,*1996] and lower than the terrestrial POC (>12) [*Hedges and Mann,* 1979; *Meyers,*1994; *Hedges et al.,* 1997; *Lamb et al.,*2006], indicating that major contribution to POC from in-situ phytoplankton production and heterotrophs rather than the terrestrial sources. The POC:Chl-*a* ratios can also be used to delineate the sources of organic matter from living resources mainly from autotrophs and heterotrophs [*Cifuentes et al.,* 1988; *Richard et al.,* 1997; *Bentaleb et al.,* 1998]. The POC:Chl-*a* ratio of fresh organic matter produced by the marine phytoplankton varies from ~40 [*Montagnes et al.,* 1994] to <200 [*Cifuentes et al.,* 1988; *Bentaleb et al.,* 1998] due to the regional differences in temperature, irradiance, growth rate and species composition [*Heath et al.,* 1990; *Montagnes et al.,* 1994; *Geider et al.,* 1998]. Heterotrophic contribution to POC pool increases the POC:Chl-*a* ratios of particulate matter because they contribute to POC but not to Chl-*a*. Mean POC:Chl-*a* ratios within the fronts of the present study (187±48), indicates that considerable amount of organic matter contribution from the phytoplankton and heterotrophy than terrestrial sources, consistent with C:N ratios.

Stable isotope ratios of C and N provide more reliable information on sources of organic matter [*Hedges et al.,* 1997] as the $\delta^{13}C$ and $\delta^{15}N$ of POC represent the isotope ratios of their source C and N, respectively [*Thunell et al.,* 2004], and have been widely used for identification of organic matter sources in marine environment [*Gearing,* 1988; *Altabet,* 1996; *Middelburg and Nieuwenhuize,*

1998; *Kuramoto and Minagawa*, 2001; *Zhang et al.,* 2007; *Sampaio et al.,* 2010; *Krishna et al.,* 2013; 2014; *Sarma et al.,* 2014]. The $\delta^{13}C_{POC}$ within the fronts (-25.7±0.4‰) are very close the range of the measured $\delta^{13}C$ of phytoplankton (-25.1±0.5‰) and zooplankton (-25.4±0.6‰) collected from the frontal regions, and enriched than the typical $\delta^{13}C$ of terrestrial particulate organic matter (-33 to -25‰) [*Barth et al.,* 1998; *Middelburg and Nieuwenhuize,* 1998]. However, the $\delta^{15}N_{PN}$ within the fronts (8.4±1.7‰) were relatively enriched than the measured $\delta^{15}N$ of phytoplankton (4.2±0.3‰) and typical $\delta^{15}N$ signatures of terrestrial organic matter (0.2-4‰) [*Thornton and McManus,* 1994], but close to the measured $\delta^{15}N$ of zooplankton (5.8±0.5‰) from frontal regions. These findings suggest that zooplankton and phytoplankton biomass predominantly contributes to the POC pool rather than the terrestrial sources.

Relatively depleted $\delta^{13}C$ and $\delta^{15}N$ of phytoplankton in the frontal regions (-25.1±0.5‰ and 4.2±0.3‰, respectively) than the typical $\delta^{13}C$ and $\delta^{15}N$ of marine phytoplankton (-23 to -21‰ and 5-7‰, respectively) [*Dehairs et al.,* 2000; *Altabet,* 1996; *Brandes and Devol.,* 2002; *Lamb et al.,* 2006] suggest that the primary production within the frontal zones is supported by the upwelling of subsurface nutrients. This is because the mineralization of organic matter by heterotrophic activity in the water column releases ^{13}C-depleted dissolved inorganic carbon (DIC) and ^{15}N-depleted dissolved inorganic nitrogen (DIN) due to the preferential release of ^{12}C and ^{14}N, respectively. The upwelling of this ^{13}C-depleted DIC and ^{15}N-depleted DIN to the surface, and their subsequent uptake by phytoplankton leads to the formation of relatively depleted $\delta^{13}C$ and $\delta^{15}N$ of phytoplankton in the frontal regions [*Altabet et al.,* 1996; *Brandes and Devol*, 2002; *Thunell et al.,* 2004; *Lamb et al.,* 2006]. Though, the $\delta^{13}C$ of DIC was not measured in this study, however, strong linear relationship between temperature and $\delta^{13}C$ of POC (depleted $\delta^{13}C$ at low temperatures) in the upper 50m of the water column of the fronts T1 (r^2=0.64, $p<0.001$), T2 (r^2=0.66, $p<0.001$), T3 (r^2=0.41, $p<0.001$), T4 (r^2=0.40, $p<0.001$) and T5 (r^2=0.39, $p<0.001$) suggest that injection of ^{13}C-depleted DIC from sub-surface to that of the surface is responsible for the depleted $\delta^{13}C_{POC}$ within the frontal regions. Measured $\delta^{13}C$ of phytoplankton also showed relatively depleted values within the fronts (-25.1±0.5‰) than the surrounding non-frontal region (-24.2±0.7‰), confirming that uptake by phytoplankton of the ^{13}C-depletd DIC in the former. Although, the slower growth rate of phytoplankton in oligotrophic waters depletes its $\delta^{13}C$ due to the relatively larger isotope fractionation during the photosynthesis reaction, however, it may not be responsible for the observed depletion in $\delta^{13}C_{POC}$ in the present study as the frontal regions are rich in nutrients.

Grazing of the $\delta^{13}C$ depleted phytoplankton by zooplankton results in further depletion of $\delta^{13}C$ in zooplankton biomass. Predominant contribution from phytoplankton and zooplankton

biomass, as indicated by C:N and POC:Chl-*a* ratios, could have also depleted the $\delta^{13}C$ of POC within the frontal regions. Intense degradation of organic matter in the frontal regions, as evident from a significant linear correlation between TBC and pCO_2 (r^2=0.43, p<0.001) and a negative relationship between TBC and dissolved oxygen (r^2=0.45, p<0.001) as mentioned previously in section 5.2, can either deplete or enrich the $\delta^{13}C$ of residual POC [*Cavagna et al.,* 2013]. However, it appears that the depleted $\delta^{13}C_{POC}$ in the present study may not be due to the bacterial modifications in $\delta^{13}C$ signatures of POC because the measured $\delta^{13}C$ of microscopically separated phytoplankton groups (unaltered by bacteria) also showed depleted $\delta^{13}C$ (-25.1±0.5‰).

Therefore, elemental C:N and POC:Chl-*a* ratios, and $\delta^{13}C$ and $\delta^{15}N$ signatures suggest that POC within the temperature fronts of the NEAS is contributed by the in-situ production and heterotrophs, with a predominance of the latter, consistent with their abundances. Significant contribution from phytoplankton biomass is mainly due to enhanced primary production supported by the nutrient input to the surface through the vertical mixing in the frontal zones, as evidenced from a linear correlation between the integrated POC and phytoplankton biomass (Chl-*a*) (r^2=0.48; p<0.001). Major contribution from heterotrophs is attributed to the intense heterotrophic activity within the fronts, as also indicated by higher TBC and zooplankton biomass, due to the availability of higher phytoplankton biomass and vertical mixing that brings TBC-rich subsurface water into the surface. However, predominant contribution from bacterial biomass may be more unlikely because POC samples were collected as the material retained on 0.7µm pore size filters. Some fraction of the bacterial biomass (of size <0.7µm) might have lost due to filtration with 0.7µm pore size filters for POC sampling. However, particle attached bacteria may contribute to the POC. Relatively deeper mixing in the open ocean fronts (63±6m) than the coastal fronts (38±8m), variable lag in the biological response to the nutrients injected into the surface [*Sarma et al.,* 2017], phytoplankton composition and the age of the front are, therefore, determining the variable contributions from in-situ production and heterotrophs to POC in the open ocean and coastal fronts. Nevertheless, this study suggests that predominant heterotrophy in the open ocean and autotrophy in the coastal ocean fronts in the northeastern Arabian Sea during winter.

Dual isotope mixing model 'SIAR' results (Table 4) revealed that predominant contributions from zooplankton biomass to POC pool within the open ocean and coastal fronts, with a proportional contribution of about 60-80% in the former and 50-60% in the latter. Contribution from phytoplankton biomass increased from open ocean (20-40%) to the coastal fronts (40-50%). Higher zooplankton contribution to POC within the open ocean fronts, and relatively higher contribution from phytoplankton within the coastal fronts (40-50%) than the open ocean fronts (20-40%) are

attributed to variable mixing depths, age of the front and phytoplankton composition in the coastal and open ocean fronts, as explained earlier. In the non-frontal regions, zooplankton and phytoplankton contribute equally in the coastal ocean, whereas it is slightly higher in the former (50-70%) than from the latter (30-50%) in the open ocean (Table 4). However, these estimations are only semi-quantitative because the two other important contributors to POC, the micro-zooplankton and bacteria, were not included in the model as end members. Since the model gives the proportional contributions, inclusion of the micro-zooplankton and bacterial end members may change these estimations. For example, relatively higher contribution from zooplankton biomass in the open ocean fronts (60-80%) than the coastal fronts (50-60%) despite the zooplankton biomass is higher by about three times in the latter (2316±930 mg m^{-2}) than that of the former (741±233 mg m^{-2}) suggesting significant contribution from micro-zooplankton in the open ocean fronts, consistent with recent observation by *Sarma et al.* [2017]. This study suggests that traditional food web is operational within the frontal zones of the coastal ocean while the microbial loop is operational in the open ocean fronts. Thus, contribution from micro-zooplankton may play a key role in the heterotrophic activity of the open ocean fronts.

Correlations between SIAR results and TBC were examined to understand the relationship of proportional contributions from phytoplankton and zooplankton to POC with that of the microbial activity. Except T2, where exceptionally higher TBC ($4.12x10^8$ Nos. l^{-1}) was found, TBC showed a strong negative correlation with phytoplankton (r^2=0.99, n=3) and a strong positive correlation with zooplankton biomass (r^2=0.99, n=3) in the frontal regions, suggesting that significant modification of POC to DOC by microbial activity and strong influence of microbial activity in the food web dynamics in the frontal regions. However, the inverse relationships of TBC with phytoplankton and zooplankton could also be due to the fact that the estimated contributions from phytoplankton and zooplankton are proportional, i. e., sum of both is 100%. Inclusion of the other two important end members, micro zooplankton and bacteria, in the SIAR model change the relative contributions from phytoplankton and zooplankton to POC, as mentioned above. However, separation of the micro-zooplankton and bacteria under microscope, and determination of their $\delta^{13}C$ and $\delta^{15}N$ ratios are still challenging and requires further efforts.

6. Summary and conclusion

A total of five temperature fronts of different ages from the coastal and open ocean regions of the northeastern Arabian Sea were investigated to understand the particulate organic carbon (POC) sources and characteristics within the fronts, and to examine their variability with space and age of the front during winter. Vertical distribution of temperature and salinity showed that upwelling of

high saline, cooler and nutrient rich waters to the surface in the frontal regions. The $\delta^{13}C$ and $\delta^{15}N$ of phytoplankton collected from surface waters of the frontal regions showed an evidence for upwelling of subsurface waters characterized by ^{13}C-depleted DIC and ^{15}N-depleted DIN to the surface in the frontal regions and supporting the biological production. Relatively higher phytoplankton biomass (Chl-*a*) was observed within the frontal regions than the surrounding non-frontal regions of all the fronts, except T1, due to availability of nutrients. The content of POC was found to be not associated with Chl-*a* and attributed to the combined influence grazing activity, decomposition of POC by heterotrophic activity and age of the front. Elemental C:N ratios, POC:Chl-*a*, $\delta^{13}C$ and $\delta^{15}N$ of particulate matter showed that predominant contribution from autotrophic and heterotrophic biomass to the POC pool. However, proportional contributions from autotrophic and heterotrophic organisms vary spatially from coastal to open ocean regions and with the age of the front. As the age of the front progresses, predominant contribution to POC shifts from autotrophic to heterotrophic organisms. Dual isotope mixing model SIAR revealed that predominant contribution to POC pool is from the zooplankton biomass within the open ocean 60-80%) than coastal (50-60%) fronts of the study region. While the contribution from phytoplankton increases from open ocean (20-40%) to coastal ocean (40-50%) fronts. Our study, therefore, suggest that open ocean fronts are dominated by heterotrophy whereas autotrophy dominates the coastal ocean fronts in the NEAS.

7. Acknowledgements

We acknowledge the Director, CSIR - National Institute of Oceanography (NIO), Goa for providing shipboard facilities, and the Scientist-In-Charge, NIO-Regional Centre, Visakhapatnam for his support and encouragement. We also thank master and his team onboard during the voyage SSK-60 for their help and support. We acknowledge Council of Scientific and Industrial Research (CSIR) for financial assistance and this work is part of the CSIR funded research project, Ocean Finder. The data used in this study was submitted to our Institute's data centre (NIODC) and can be archived from http://www.nio.org/iodc. This publication has NIO contribution number .....

8. References

Altabet, M. (1996), Nitrogen and carbon isotopic tracers of the source and transformation of particles in the deep sea. In: Ittekkot, V., P. Schaefer, S. Honjo, P.J. Depetris, (ed) Particle flux in the Ocean. SCOPE, Vol, 57, Wiley & Sons, Chichester, pp. 155-184.

Amol, P., D. Shankar, V. Fernando, A. Mukherjee, S. G. Aparna, R. Fernandes, G. S. Michael, S. T. Khalap, N. P. Satelkar, Y. Agarvedekar, M. G. Gaonkar, A. P. Tari, A. Kankonkar and S. P. Vernekar (2014), Observed intraseasonal and seasonal variabilityof the West India Coastal Current on the continental slope, *J. Earth Syst. Sci. 123*, 1045–1074.

Armstrong, D. A., B. A. Mitchell-Innes, F. Verheye-Dua, H. Waldron and L. Hutchings (1987), Physical and biological features across an upwelling front in the southern Benguela, *South African J. Mar. Sci., 5,* 171-190.

Asaro, D. E., C. Lee, L. Rainville, R. Harcourt, and L. Thomas (2011), Enhanced turbulence and energy dissipation at ocean fronts, *Science, 332* (6027), 318.

Bang, N. D. (1973), Characteristics of an intense ocean frontal system in the upwell regime west of Cape Town, *Tellus, 25,* 256-265.

Banse, K. (1968), Hydrography of the Arabian Sea shelf of India and Pakistan and effects on demersal fishes, *Deep-Sea Res., 15,* 45–79.

Banse, K. (1984), Overview of the hydrography and associated biological phenomena in theArabian Sea, off Pakistan. In: Huq, B. U. and J. D. Milliman (Eds.), *Marine Geology and Oceanography of Arabian Sea and Coastal Waters.* Van Nostrand Reinhold Co., N.Y., pp. 271–303.

Banse, K., and C. R. McClain (1986), Winter blooms of phytoplankton in the Arabian Sea as observed by the Coastal Zone Color Scanner, *Mar. Ecol. Progr. Ser., 34,* 201-211.

Barber, R. T., J. Marra, R. C. Bidigare, L. A. Codispoti, D. Halpern, Z. Johnson, M. Latasa, R. Goericke, and S. L. Smith (2001), Primary productivityand its regulation in the Arabian Sea during 1995, *Deep Sea Res., Part II, 48,* 1127–1172.

Barth, J. A. C., J. Veizer, B. Mayer (1998), Origin of particulate organic carbon in the upper St. Lawrence: Isotopic constraints, *Earth Planet. Sci. Lett., 162*, 111-121.

Barton, E. D., A. Huyer, and R. L. Smith (1977), Temporal variation observed in the hydrographic regime near Cabo Corveiro in the northwest African upwelling region, February to April 1974, *Deep Sea Res., 24,* 7-23.

Behrenfeld, M. J. (2010), Abandoning Sverdrup's Critical Depth Hypothesis on phytoplankton blooms, *Ecology, 91,* 977–989.

Belkin, I. M., and P. C. Cornillon (2005), Bering Sea thermal fronts from pathfinder data: seasonal and inter annual variability, *Pac. Oceanogr., 3,* 6–20.

Belkin, I. M., P. C. Cornillon, and K. Sherman (2009), Fronts in large marine ecosystems, *Prog. Oceanogr., 81,* 223–236.

Bentaleb, I., M Fontugne, C. Descolas-Gros, C. Girardin, A. Mariotti, C.Pierre,C. Brunet, and A. Poisson (1998), Carbon isotopicfractionation by plankton in the Southern Indian Ocean: relation between $\delta^{13}C$ of particulate organic carbon and dissolved carbon dioxide, *J. Mar. Sys., 17,* 39–58.

Brandes, J. A., and A. H. Devol (2002), A global marine-fixed nitrogen isotopic budget: implications for Holocene nitrogen cycling, *Glob. Biogeochem. Cy.*, doi: 10.1029/2001GB001856.

Carritt, D. E., and J. H. Carpenter (1966), Comparison and evaluation of currently employed modifications of Winkler method for determining dissolved oxygen in seawater a Nasco report, *J. Mar. Res., 24,* 286.

Cavagna, A. –J., F. Dehairs, S. Bouillon, V. Woule-Ebongue, F. Planchon, B. Delille, and I Bouloubasssi (2013), Water column distribution and carbon isotopic signal of holesterol, brassicasterol and particulate organic carbon in the Atlantic sector of the Southern Ocean, *Biogeosciences, 10,* 2787–2801.

Cifuentes, L. A., J. H. Sharp, and M. L. Fogel (1988), Stable carbon and nitrogen isotope biogeochemistry in the Delaware estuary, *Limnol. Oceanogr., 33,* 1102–1115.Colton, J. B. Jr., D. E. Smith, and J. W. Jossi (1975), Further observations on a thermal front in the Sargasso Sea, *Deep-sea Res., 22,* 433-439.

Créach, V. (1995), Origin eset transferts de la matièreorganiquedans un marais littoral: utilisation des compositeons isotopiques naturelles du carbone et de l'azote. PhD thesis, Université de Rennes I—Muséumd'Histoire Naturelle, Rennes

Csanady, G. T. (1982), Circulation in the Coastal Ocean. Boston: Reidel Publishing Co., pp. 280.

Dehairs, F., R. G. Rao, P. Chandra Mohan, A. V. Raman, S. Marguillier, L. Hellings (2000), Tracing mangrove carbon in suspended matter and aquatic fauna of the Gautami-Godavari delta, Bay of Bengal (India), *Hydrobiology 431,* 225-241.

Dengler, A. T. (1985), Relationship between physical and biological processes at an upwelling front off Peru, 15^{o}S, *Deep-Sea Res., 32,* 1301-1315.

Dong, S., S. T. Gille, J. Sprintall, and C.Gentlemann, (2006), Validation of the advanced microwave scanning radiometer for the earth observing system (AMSR-E) sea surface temperature in the Southern Ocean, *J. Geophys. Res. 111,* C04002

Dubois, S., N. Savoye, A. Grémare, M. Plus, K. Charlier, A. Beltoise, and H. Blanchet (2012), Origin and composition of sediment organic matter in a coastal semi-enclosed ecosystem: An elemental and isotopic study at the ecosystem space scale, *J. Mar. Sys., 94,* 64-73.

Fagerbakke, K. M., M. Heldal, and S. Norland (1996), Content of carbon, nitrogen, oxygen, sulfur and phosphorus in native aquatic and cultured bacteria, *Aquat. Microb. Ecol., 10,* 15–27.

Fox-Kemper, B., R. Ferrari, and R. Hallberg (2008), Parameterization of mixed layer eddies. Part I: Theory and diagnosis, *J. Phys. Oceanogr., 38,* 1145–1165.

Franks, P. J. S. (1992), Phytoplankton blooms at fronts: Patterns, scales, and physical forcing mechanisms, *Rev. Aquat. Sci., 6,* 121-137.

Gauns M., M. Madhupratap, N. Ramaiah, R. Jyothibabu, V. Fernandes, J. T. Paul and S. Prasanna Kumar (2005), Comparative accounts of biological productivity characteristics and estimates of carbon fluxes in the Arabian Sea and the Bay of Bengal, *Deep Sea Res. Part II,* 52, 2003–2017.

Gearing, J. N (1988), The use of stable isotope ratios for tracing the near shore-offshore exchange of organic matter. Lecture notes on coastal and estuarine studies, vol. 22. In: Jansson, B.O., (Ed.), Coastal Offshore Ecosystem Interactions. Springer-Verlag, NewYork, pp. 69-101.

Geider, R. J., H. L. McIntyre, and T. M. Kana (1998), A dynamic regulatory model of phytoplanktonic acclimation to light, nutrients, and temperature, *Limnol. Oceanogr., 43,* 679–694.

Grashoff, K., M. Ehrhardt, and K. Kremling (1992), Methods of Seawater Analysis, 419 pp., Verlag Chemie, New York.

Halpern, D. (1976), Structure of a coastal upwelling event observed off Oregon during July 1973, *Deep Sea Res., 23,* 495-508.

Haynes, R., E. D. Barton and I. Pilling (1993), Development, persistence and variability of upwelling filaments off the Atlantic Coast of the Iberian Peninsula, *J. Geophys. Res., 98,* 22681–22692.

Heath, M. R., K. Richardson, and T. Kiørboe (1990), Optical assessment of phytoplankton nutrient depletion, *J. Plankton. Res. 12,* 381–396.

Hedges, J. I., R. G. Keil, and R. Benner (1997), What happens to terrestrial organic matter in the ocean? *Org. Geochem., 27,* 195–212.

Hedges, J. I., and D. C. Mann (1979), The characterization of plant tissues by their lignin oxidation products, *Geochim. Cosmochim. Acta 43,* 1803–1807.

Hesse, K. J., Z. L. Liu, and K. Schaumann, (1989), Phytoplankton and fronts in the German Bight, *Sci. Mar. 53,* 187–196.

Hickox, R., I. M. Belkin, P. C. Comillon and Z. Shan (2000), Climatology and seasonal variabililty of ocean fronts in the East China, Yellow, and Bohai Seas from satellite SST data, *Geophys. Res. Lett., 27,* 2945-2948.

Holligan, P. M., P. Le, B. Williams, D. Purdee, and R. Harris (1984a), Photosynthesis, respiration and nitrogen supply of plankton populations in stratified, frontal and tidally mixed shelf waters, *Mar. Ecol. Prog. Ser., 17,* 201-213.

Holligan, P. M., R. P. Harris, R. C. Newell, D. S. Harbour, R. N. Head, E. A. S. Linley, M. I. Lucas, P. R. G. Tranter, and C. M. Weekley, (1984b), Vertical distribution and partitioning of organic carbon in mixed, frontal, stratified waters of the English Channel, *Mar. Ecol. Prog. Ser., 14,* 111-127.

Hulbert, E. M. (1964), Succession and diversity in the planktonic flora of the western North Atlantic. *Bull. Mar. Sci. Gulf and Caribbean 14,* 3344.

Jackson, A. L., R. Inger, S. Bearhop, and A. Parnell (2009), Erroneous behaviour of MixSIR, a recently published Bayesian isotope mixing model: a discussion of Moore & Semmens, Ecology Letters, 2008. Ecology Letters 12: E1–E5.

Jennerjahn, T. C., V. Ittekkot, S. Klopper, S. Adi, S. P. Nugroho, N. Sudiana ,A. Yusmal, Prinhartanto, and B. Gaye-Haake (2004), Biogeochemistry of a tropical river affected by human activity in its catchment: Brantas River estuary and coastal waters of Madura Strait. Java, Indonesia, *Estuar. Coast Shelf. Sci., 60,* 503-514.

Khandeparker, L., R. Easwaran, L. Garade, N. Kuchi, K. Mapari, S. D. Naik and A. C. Anil (2017), Elucidation of the tidal influence on bacterial populations in a monsoon influenced estuary through simultaneous observations, *Environ. Mon. Assess., 189,* 41, https://doi.org/10.1007/s10661-016-5687-3

Koski, M. (1999), Carbon:nitrogen ratios of Baltic Sea copepods - indication of mineral limitation? *J. Plankton Res. 21,* 1565–1573.

Krishna, M. S., S. A. Naidu, Ch. V. Subbaiah, V. V. S. S. Sarma, and N. P. C. Reddy (2013), Distribution and sources of organic matter in surface sediments of the eastern continental margin of India, *J. Geophys. Res. Biogeosci. 118*,doi:10.1002/2013JG002424.

Krishna, M. S., S. A. Naidu, Ch. V. Subbaiah, G. Lata, V. V. S. S. Sarma, and N. P. C. Reddy (2014), Source, distribution and preservation of organic matter in a tropical estuary (Godavari, India), *Estuar. Coasts*, doi: 10.1007/s12237-014-9859-5

Kumar, S. P., R. P. Roshin, J. Narvekar, P. K. D. Kumar, and E. Vivekanandan (2010), What drives increased phytoplankton biomass in the Arabian Sea, *Curr Sci., 99,* 101-106.

Kuramoto, T. and M. Minagawa, (2001), Stable Carbon and Nitrogen Isotopic characterization of Organic Matter in a Mangrove Ecosystem on the Southwestern Coast of Thailand, *J. Oceanogr. 57,* 421-431.

Lamb, A. L., G. P. Wilson, and M. J. Leng (2006), A review of coastal palaeoclimate and relative sea-level reconstructions using $\delta^{13}C$ and C/N ratios in organic material, *Earth Sci. Rev., 75,* 29–57.

Le Fèvre-Lehoerff, G., E. Erard-le Denn, and G.Arzul (1993), Planktonic ecosystems in the Channel: trophic relations, *Oceanol. Acta 16,* 661–670.

Levy, M., P. Klein, and A. Treguier (2001). Impact of sub-meso scale physics on production and subduction of phytoplankton in an oligotrophic regime, *J. Mar. Res., 59,* 535-565.

Li, Q. P., P. J. S. Franks, M. D. Ohman, and M. R. Landry (2012), Enhanced nitrate fluxes and biological processes at a frontal zone in the southern California current system. *J Plankton Res*., *34*, 790–801.Madhupratap, M., S. Prasanna Kumar, P. M. A. Bhattathiri, S. Raghukumar, K. K. C. Nair, and N. Ramaiah (1996), Mechanism of biological response to winter cooling in the northeastern Arabian Sea, *Lett. Nat., 384,* 549–552.

Mahadevan, A., A. Tandon, and R. Ferrari (2010), Rapid changes in mixed layer stratification driven by sub meso-scale instabilities and winds, *J. Geophys. Res., 115,* C03017, doi:10.1029/2008JC005203.

Mahadevan, A., and A. Tandon (2006), An analysis of mechanisms for sub meso-scale vertical motion at ocean fronts, *Ocean Modell., 14,* 241–256.

Mahadevan, A., and D. Archer (2000), Modeling the impact of fronts and meso-scale circulation on the nutrient supply and biogeochemistry of the upper ocean, *J. Geophys. Res.*, *105* (C1), 1209–1225.

Mahadevan, A., L. Thomas, and A. Tandon (2008), Comment on Eddy/wind interactions stimulate extraordinary mid-ocean plankton blooms, *Science, 320* (5875), 448.

McCreary, J. P., K. E. Kohler, R. R. Hood and D. B. Olson (1996), A four-component ecosystem model of biological activity in the Arabian Sea, *Prog. Oceanogr., 37,* 193-240.

McCreary, J. P., R. Murtugudde, J. Vialard, P. N. Vinayachandran, J. D. Wiggert, R. R. Hood, D. Shankar and S. R. Shetye (2009), Biophysical processes in the Indian Ocean, *Geophys. Monogr. Ser. 185*, 9–32.

Meyers, P. A. (1994), Preservation of elemental and isotopic source identification of sedimentary organic matter, *Chem. Geol. 144*, 289–302.

Middelburg, J. J., and J. Nieuwenhuize (1998), Carbon and nitrogen stable isotopes in suspended matter and sediments from the Schelde estuary, *Mar. Chem., 60,* 217-225.

Montagnes, D. J. S., J. A. Berges, P. J. Harrison, and F. J. R. Taylor (1994), Estimating carbon, nitrogen, protein and chlorophyll *a* from volume in marine phytoplankton, *Limnol. Oceanogr., 39*,1044–1060.

Moore, J. K., M. R. Abbot, and J. G. Richman (1999), Location and dynamics of the Antarctic polar front from satellite sea surface temperature data, *J. Geophys. Res., 104*, 3059–3073.

Muraleedharan, P. M. and S. Prasanna Kumar (1996), Arabian Sea upwelling—A comparison between coastal and open ocean regions, *Curr. Sci., 71*, 842–846.

Naqvi, S. W. A., V. V. S. S. Sarma, and D. A. Jayakumar (2002), Carbon cycling in the northern Arabian Sea during the northeast monsoon: Significance of salps, *Mar. Ecol. Progr. Ser., 226*, 35–44.

Oguz, T., D. Macías, and J. Tintoré (2014), Impacts of boundary current instabilities on plankton production characteristics of the Catalano-Balearic Sea (Western Mediterranean), Ocean Model.

Obenour, K. M. (2014), Temporal Trends in Global Sea Surface Temperature Fronts. OpenAccess Master's Theses.

Ohman, M. D., J. R. Powell , M. Picheral, and D. W. Jensen (2012), Meso-zooplankton and particulate matter responses to a deep-water frontal system in the southern California Current System, *J Plankton Res., 34*, 815–827.

Olita, A., S. Sparnocchia, S. Cusí, L. Fazioli, R. Sorgente, J. Tintoré, and A. Ribotti (2014), Observations of a phytoplankton spring bloom onset triggered by a density front in NW Mediterranean, *Ocean Sci., 10*, 657–666.

Onstad, G. D., D. E. Canfield, P. D. Quay and J. I. Hedges (2000), Sources of particulate organic matter in rivers from the continental USA: lignin phenol and stable carbon isotope compositions, *Geochim. Cosmochim. Acta 64*, 3539-3546.

Owen, R. W. (1981), Fronts and eddies in the sea: mechanisms interactions and biological effects. In *Analysis of Marin~ Ecosystems*. Longhurst, A. R. (Ed.). London; Academic Press: 197-233Park, S. and P. C. Chu (2006), Thermal and haline fronts in the Yellow/East China Seas: surface and subsurface seasonality comparison, *J. Oceanogr. 62*, 617–638.

Parnell, A., R. Inger, S. Bearhop, and A. L. Jackson (2008), SIAR: Stable Isotope Analysis in R. http://cran.r-roject.org/web/packages/siar/index.html

Parnell. A., R. Inger, S. Bearhop, and A.L. Jackson, (2010), Source partitioning using stable isotopes coping with too much variation, *Plos One 5*, 9672.

Pollard, R. T. and L. A. Regier (1990), Large variations in potential vorticity at small scales in the upper ocean, *Nature, 348*, 227-229.

Prasanna Kumar, S. and T. G. Prasad (1996), Winter cooling in the northern Arabian Sea, *Curr. Sci., 71,* 834-841.

Ramp, S. R., P. F. Jessen, K. H. Brink, P. P. Niiler, F. L. Daggett and J. S. Best (1991), The physical structure of cold filaments near Point Arena, California, during June 1987, *J. Geophys. Res., 96,* 14859–14883.

Randerson, J. T. and J. J. Simpson (1993), Recurrent patterns in surface thermal fronts associated with cold filaments along the west coast of North America. Remote Sens, *Environ. 46,* 146–163.

Redfield, A. C., B. H. Ketchum, and F. A. Richards (1963), The influence of organisms on the composition of seawater, In: The sea, vol. 2, ed. M.N. Hill, 26–77. New York: Wiley.

Richard, P., P. Riera, and R. Galois (1997), Temporal variations in the chemical and carbon isotope compositions of marine and terrestrial organic inputs in the bay of Marennes-Oléron, France, *J. Coast Res. 13,* 879–899.

Roy, R., A. K. Prathihary, G. Mangesh, S. W. A. Naqvi (2006), Spatial variation of phytoplankton pigments along the southwest coast of India, *Estuar.Coast. Shelf Sci. 69,* 189–195.

Roy, R., C. Rajath, K. Vinayak, M. S. Krishna, V. V. S. S. Sarma, and A. C. Anil (2015), CHEMTAX-derived phytoplankton community structure associated with temperature fronts in the northeastern Arabian Sea, *J. Mar. Syst., 144,* 81-91.

Rudnick, D. L. and J. R. Luyten (1996), Intensive survey of the Azores front: 1. Tracers and dynamics, *J. Geophys. Res., 101,* 923-939.

Sampaio, L., R. Freitas, C. Maguas, A. Rodrigues, and V. Quintino (2010), Coastal sediments under the influence of multiple organic enrichment sources: An evaluation using carbon and nitrogen stable isotope, *Mar. Poll. Bull. 60,* 272-282.

Sardessai, S., V. V. S. S. Sarma, M. Dileep Kumar (1999), Particulate organic carbon and particulate humic material in the Arabian Sea, *Ind. J. Mar. Sci., 28,* 5-9.

Sarma, V. V. S. S., J. Arya, Ch. V. Subbaiah, S. A. Naidu, L. Gawade, P. P. Kumar, and N. P. C. Reddy (2012), Stable isotopes of carbon and nitrogen in suspended matter and sediments from the Godavari estuary, *J. Oceanogr. 68,* 307-319.

Sarma, V. V. S. S., M. S. Krishna, V. R. Prasad, B. S. K. Kumar, S. A. Naidu, G. D. Rao, R. Viswanadham, T. Sridevi, P. P. Kumar, N. P. C. Reddy (2014), Distribution and sources of particulate organic matter in the Indian monsoonal estuaries during monsoon, *J. Geophys. Res. Biogeosci., 119,*doi:10.1002/2014JG002721.

Sarma, V. V. S. S., H. B. Delabehera, P. Sudharani, R. Remya, J. S. Patil, and D. Dessai (2015), Variations in the inorganic carbon components in the thermal fronts during winter in the northeastern Arabian Sea, *Mar. Chem., 169,* 16-22.

Sarma, V. V. S. S., D. V. Desai, J. S. Patil, L. Khandeparker, S. G. Aparna, D. Shankar, Selrina D'Souza, H. B. Dalabehera, J. Mukherjee, P. Sudharani and A.C. Anil (2017), Ecosystem response in temperature fronts in the northeastern Arabian Sea, accepted in *Progress in Oceangraphy*.

Schoemann, V., S. Becquevort, J. Stefels, V. Rousseau and C. Lancelot (2005), Phaeocystisblooms in the global ocean and their controlling mechanisms: a review, *J. Sea Res. 53,* 43-66.

Shannon, L. V. (1985), The Benguela ecosystem. I. Evolution of the Benguela, physical features and processes. In: Barnes, M. (Ed), *Oceanography and Marine Biology. An annual Review 23*, 105-182, Aberdeen: University Press.

Shetye, S. R. (1998), West India coastal current and Lakshadweep high/low, *Sadhana, 23*,637–651.

Shetye, S. R., A. D. Gouveia and S. S. C. Shenoi (1994), Circulation and water masses of the Arabian Sea. *Proc. Ind. Acad. Sci.-Ear. Planet. Sci., 103*, 107-123.

Smith, S. L. (2001), Understanding the Arabian Sea: Reflections on the 1994–1996 Arabian Sea Expedition, *Deep Sea Res., II, 48*, 1385– 1402.

Smith, W. O., C. A. Carlson, H. W. Ducklow, and D. A. Hansell (1998), Growth dynamics of Phaeocystis antarctica-dominated plankton assemblages from the Ross Sea, *Mar. Ecol. Prog. Ser., 168*, 229–244.

Smyth, T. J., P. I. Miller, S. B. Groom and S. J. Lavender (2001), Remote sensing of sea surface temperature and chlorophyll during Lagrangian experiments at the Iberian margin, *Prog. Oceanogr. 51,* 269–281.

Solanki, H. U., R. M. Dwivedi, S. R. Nayak, V. S. Somvanshi, D. K. Gulati, and S. K. Pattnayak (2003), Fishery forecast using OCM chlorophyll concentration and AVHRR SST: validation results off Gujarat coast, India, *Int. J. Remote Sensing, 24,* 3691-3699.

Solanki, H. U., P. C. Mandoki, S. R. Nayak, and V. S. Somvanshi (2005), Evaluation of remote sensing-based potential fishing zones (PFZs) forecast methodology, *Cont. Shelf Res., 25,* 2163–2173.

Strub, P. T., P. M. Kosro and A. Huyer (1991), The nature of the cold filaments in the CaliforniaCurrent System, *J. Geophys. Res., 96*, 14743–14768.

Stukel et al., (2017), Mesoscale ocean fronts enhance carbon export due to gravitational sinking and subduction, *Proc. Nat. Acad. Sci.,114*, 1252-1257.

Taylor, J. R. and R. Ferrari (2011), Ocean fronts trigger high latitude phytoplankton blooms, *Geophys. Res. Letters., 38,* doi: 10.1029/2011GL049312.

Taylor, J. and R. Ferrari (2010), Buoyancy and wind-driven convection at a mixed-layer density fronts, *J. Phys. Oceanogr.*, 40, 1222–1242.

Taylor, J. and R. Ferrari (2010), Shutdown of turbulent convection as a new criterion for the onset of spring phytoplankton blooms, *Limnol. Oceanogr., 56,* 2293–2307, doi:10.4319/lo.2011.56.6.2293.

Thomas, L. N. and J. R. Taylor (2010), Reduction of the usable wind-work on the general circulation by forced symmetric instability, *Geophys. Res. Lett., 37*, L18606, doi:10.1029/2010GL044680.

Thornton, S. F. and J. McManus (1994), Application of organic carbon and nitrogen stable isotope and C/N ratios as source indicators of organic matter provenance in estuarine systems: Evidence from the Tay Estuary. Scotland, *Estuar. Coast. Shelf Sci., 38,* 219–233.

Thunell, R. C., D. M. Sigman, F. Müller-Karger, Y. Astor, and R. Vareka (2004), Nitrogen isotopic dynamics of the Cariaco Basin, Venezuela, *Glob. Biogeochem. Cy.,* doi:10.1029/2003GB002185.

Thurman, H. and A. Trujillo (1999), Essentials of Oceanography, Prentice Hall, Upper Saddle River, N. J.

Traganza, E. D., D. G. Redalje, and R. W. Garwood (1987), Chemical flux, mixed layer entrainment and phytoplankton blooms at upwelling fronts in the California coastal zone, *Cont. Shelf Res., 7*, 89-105.

Unnikrishnan, A. S. and M. K. Antony (1992), On an upwelling front along the west coast of India during later part of southwest monsoon, *Phys. Process. Indian Seas* 131–135.

Van Heukelem, L. (2002). HPLC phytoplankton pigments: sampling, laboratory methods, and quality assurance procedures. In: Mueller, J. and G. Fargion (Eds.), Ocean Optics Protocols for Satellite Ocean Color Sensor, Revision 3, Volume 2,Chapter16,NASA Technical Memorandum 2002–2004. Volume 2, pp. 258–268.

Vipin, P., K. Sarkar, S. G. Aparna, D. Shankar, V. V. S. S. Sarma, D. G. Gracias, M. S. Krishna, G. Srikanth, B. Mandal, E. P. Rama Rao, and N. Srinivasa Rao, (2015), Evolution and sub-surface characteristics of an SST Filament and Front in the Northeastern Arabian Sea during November-December 2012, *J. Mar. Syst., 150*, 1-11.

Wu, J. P., S. E. Calvert, and C. S. Wong (1997), Nitrogen isotope variations in the subarctic northeast Pacific: relationships to nitrate utilization and trophic structure. *Deep-Sea Res., 44*, 287-314.

Wu, J. P., S. E. Calvert, C. S. Wong, and F. A. Whitney (1998), Carbon and nitrogen stable isotope variations in sedimentary organic matter from the Ross Sea, Antarctica: A record of phytoplankton bloom Pacific, *J. Plankton Res., 17,* 439-464.

Wyrtki, K. (1971), Oceanographic Atlas of the International Indian Ocean Expedition.National Science Foundation, Washington, D. C.

Yoder, J. A., S. G. Ackleson, R. Barber, et al. (1994), A line in the sea, *Nature*, *371,* 689-692.

Zhang, J., Y. Wu, Jennerjahn, V. Ittekkot, Q, He, (2007), Distribution of organic matter in the Changjiang (Yangtze River) estuary and their stable carbon and nitrogen isotopic ratios: Implications for source discrimination and sedimentary dynamics, *Mar. Chem., 106,* 111-126.

Figure Captions

Figure 1: Map showing the Arabian Sea, the northwestern Indian Ocean. The inset box shows the region investigated during this study in the northeastern Arabian Sea (NEAS). The expansion of the box in the map shows the average SST (°C) during the sampling period (24-30 January 2014). Transects sampled (T1 to T5) were shown by solid black lines while the station locations were shown by filled black squares. Starting station of each transect was shown by the alphabet 'a' and increases the station numbers with ascending alphabets. For instance, T1a and T1j indicate the first and last stations on Transect 1. Only in the case of transect T2, starting station 'a' is not at the end of transect. Initially samples were collected at T2a to capture the front and then moved to northwest direction and sampled T2b following T2c and T2d. The PFZ advisories given by INCOIS on different dates during our sampling period (24-30 January, 2014) in the NEAS were also marked. Different color of the curves indicates the PFZ advisory on different dates.

Figure 2: Horizontal and vertical distribution of (a) temperature (^{o}C), (b) salinity, (c) chlorophyll-a (mg m^{-3}), (d) particulate organic carbon (µM L^{-1}) and (e) particulate nitrogen(µM L^{-1}) in temperature fronts T1, T2, T3, T4 and T5 in the north eastern Arabian Sea during winter. X- axis refers to the distance computed from northwest to southeast for fronts T1 and T2, and from west to east for T3, T4 and T5. The sampling was done in an opposite direction for fronts T3 and T5.

Figure 3: Horizontal and vertical distribution of (a) stable isotope ratio of particulate organic carbon ($\delta^{13}C_{POC}$, ‰), (b) stable isotope ratio of particulate nitrogen ($\delta^{15}N_{PN}$, ‰) and (c) elemental carbon to nitrogen ratio (C:N) in temperature fronts T1, T2, T3, T4 and T5 in the north eastern Arabian Sea during winter. X-axis refers to the distance computed for different fronts as given in caption of Fig. 2.

Table Captions

Table 1: Difference between within the front (frontal) and outside the front (non-frontal) regions in temperature (^{o}C) and integrated content of phytoplankton biomass (Chlorophyll-a; mg m^{-2}), particulate organic carbon (POC, mg m^{-2}) and particulate nitrogen (PN, mg m^{-2}) in elemental C:N ratio and POC:Chl-*a* ratios in surface 50m of water column of the fronts T1, T2,T3, T4 and T5 in the northeastern Arabian Sea.

Table 2: Variability in the mean stable carbon and nitrogen isotopes of particulate organic carbon ($\delta^{13}C_{POC}$ and $\delta^{15}N_{PN}$, ‰ respectively), phytoplankton groups ($\delta^{13}C_{PHYTO}$ and $\delta^{15}N_{PHYTO}$, ‰) and Zooplankton groups ($\delta^{13}C_{ZOO}$ and $\delta^{15}N_{ZOO}$, ‰) collected within the frontal (F) and non-frontal (NF) regions of T1, T2, T3 and T4 in the northeastern Arabian Sea

Table 3: Probability associated with the two-sample equal variance (homoscedastic) Student's t-Test, with a two tailed distribution, between the frontal and non-frontal regions of integrated particulate organic carbon (Int. POC), particulate nitrogen (Int. PN) and chlorophyll-a (Int. Chl-a), and POC:Chl-a, $\delta^{13}C$ and $\delta^{15}N$ ratios of suspended particulate organic matter. Asterisk (∗) indicates significant p value ($p<0.01$) for $\delta^{15}N$ values between the frontal and non-frontal regions of the fronts T4 and T5.

Table 4: Proportional contributions of organic matter from phytoplankton and zooplankton to suspended particulate organic matter in the frontal and non-frontal regions of T1, T2, T3 and T4 fronts in the northeastern Arabian Sea during winter.

Transect	Temperature (°C)		Chlorophyll-a (mg m^{-2})		POC (µg m^{-2})		PN (µg m^{-2})		Zooplankton biomass (mg m^{-2})		C:N ratio		POC:Chl-a	
	F	NF	F	NF	F	NF	F	NF	F	NF	F	NF	F	NF
T1	24.8	25.2	30.1	31.5	5352	4704	941	957	576	177	6.7	7.5	162	192
T2	23.8	25.4	67.9	31.6	5159	5253	1014	1190	906	480	6.7	5.0	225	213
T3	24.7	25.3	36.2	27.8	4623	4729	1367	1230	1919	1154	4.6	4.9	141	191
T4	24.6	25.2	27.4	23.2	5144	5916	1354	1313	3379	1258	5.8	4.9	253	195
T5	24.5	24.9	44.1	18.2	6591	6144	1323	1222	1649	1137	5.6	6.0	157	205

Table 1

Transect	$\delta^{13}C_{POC}$ (‰)		$\delta^{13}C_{PHYTO}$ (‰)		$\delta^{13}C_{ZOO}$ (‰)		$\delta^{15}N_{PN}$ (‰)		$\delta^{15}N_{PHYTO}$ (‰)		$\delta^{15}N_{ZOO}$ (‰)	
	F	NF	F	NF	F	NF	F	NF	F	NF	F	NF
T1	-25.2	-24.5	-22.3	-24.3	-24.7	-24.6	8.8	20.0	4.5	4.1	5.8	4.9
T2	-26.1	-25.5	-24.6	-23.4	-26.1	-24.7	6.4	7.7	4.5	4.0	6.1	5.0
T3	-24.6	-25.1	-25.6	-25.1	-25.7	-24.7	10.5	14.9	3.9	3.5	6.1	6.1
T4	-25.3	-25.7	-25.1	-24.1	-24.9	-24.4	10.5	10.0	4.0	3.5	5.0	5.1

Table 2

Front	Int. POC	Int. PN	Int. Chl-a	POC:Chl-a	$\delta^{13}C$	$\delta^{15}N$
T1	0.63	0.61	0.48	0.57	0.08	0.03
T2	-	-	-	0.84	0.25	0.42
T3	0.12	0.87	0.01	0.39	0.49	0.02
T4	0.79	0.65	1.00	0.22	0.20	0.00*
T5	0.60	0.57	0.79	0.12	0.19	0.00*

*: $p<0.01$, -: not performed as only one station was sampled within the front

Table 3:

Front	Front		non-front	
	Phyto (%)	Zoo (%)	Phyto (%)	Zoo (%)
T1	20	80	50	50
T2	40	60	30	70
T3	40	60	45	45
T4	50	50	30	70

Table 4:

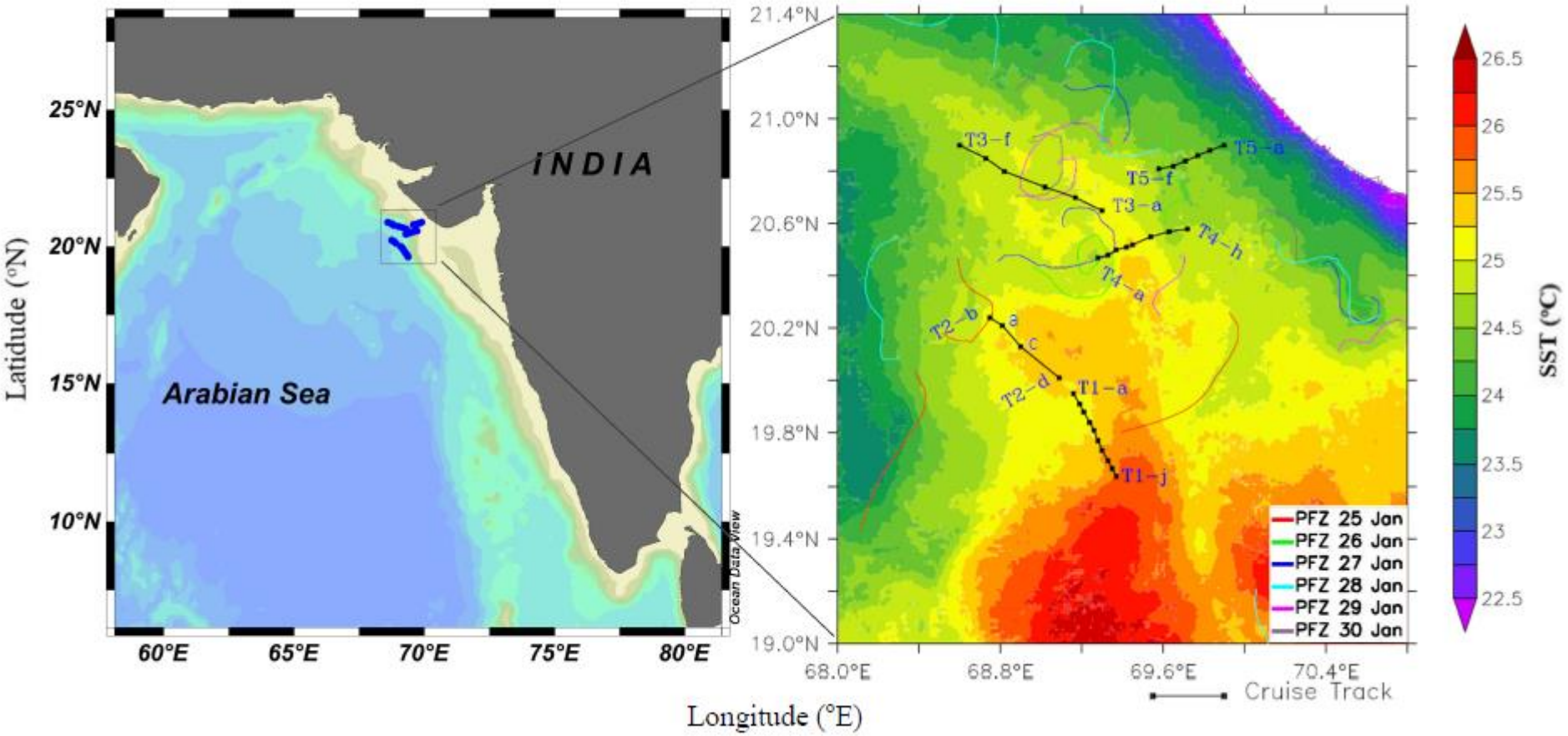
INDIA
Arabian Sea
25°N
20°N
15°N
10°N
60°E
65°E
70°E
75°E
80°E
Latitude (°N)
Longitude (°E)
Ocean Data View
21.4°N
21.0°N
20.6°N
20.2°N
19.8°N
19.4°N
19.0°N
68.0°E
68.8°E
69.6°E
70.4°E
T3 – f
T5 – e
T5 – f
T3 – a
T4 – h
T4 – a
T2 – b
a
c
T2 – d
T1 – a
T1 – j
PFZ 25 Jan
PFZ 26 Jan
PFZ 27 Jan
PFZ 28 Jan
PFZ 29 Jan
PFZ 30 Jan
Cruise Track
26.5
26
25.5
25
24.5
24
23.5
23
22.5
SST (°C)

Fig. 1

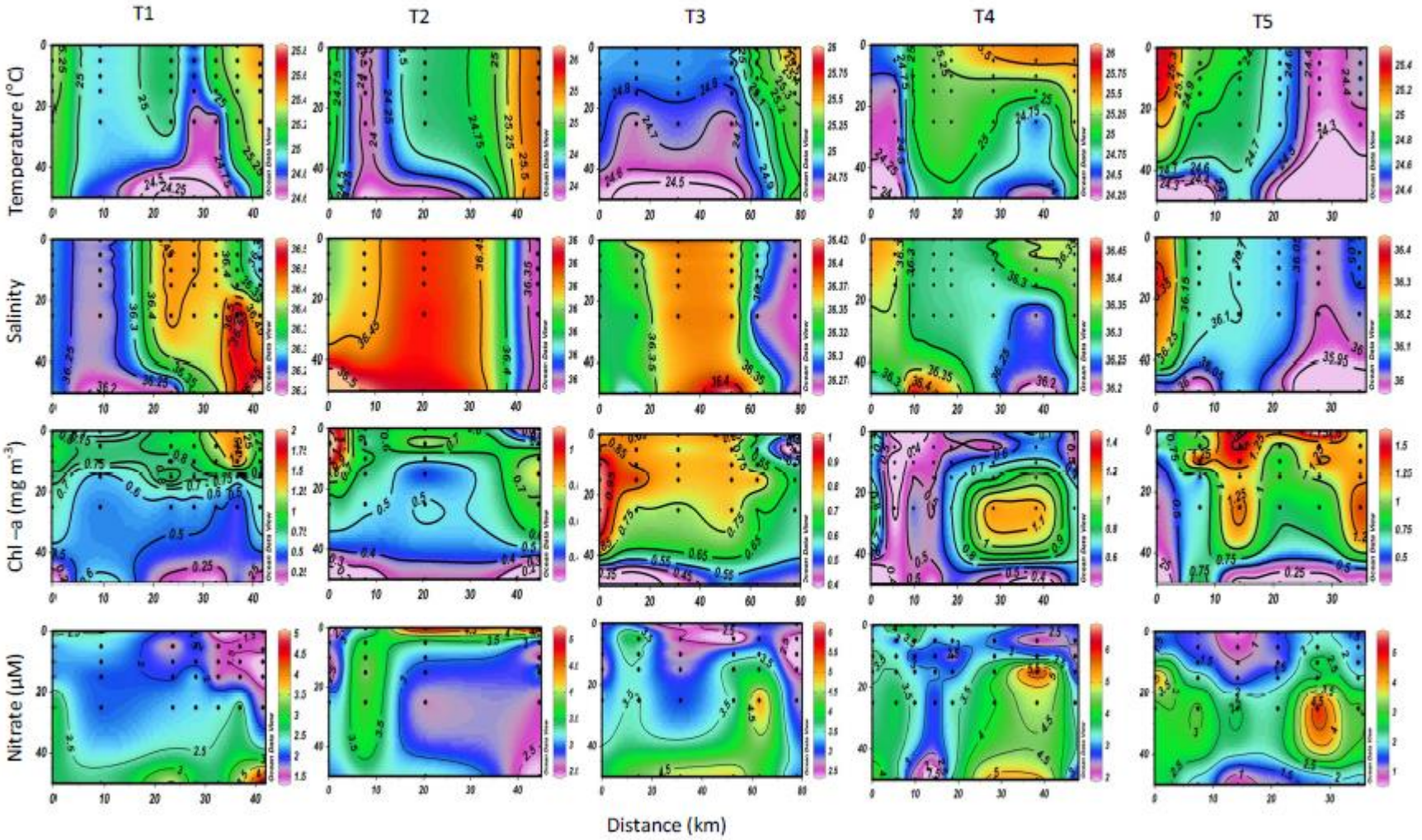
T1
T2
T3
T4
T5
Temperature (°C)
Salinity
Chl –a (mg m-3)
Nitrate (µM)
Distance (km)

Fig. 2

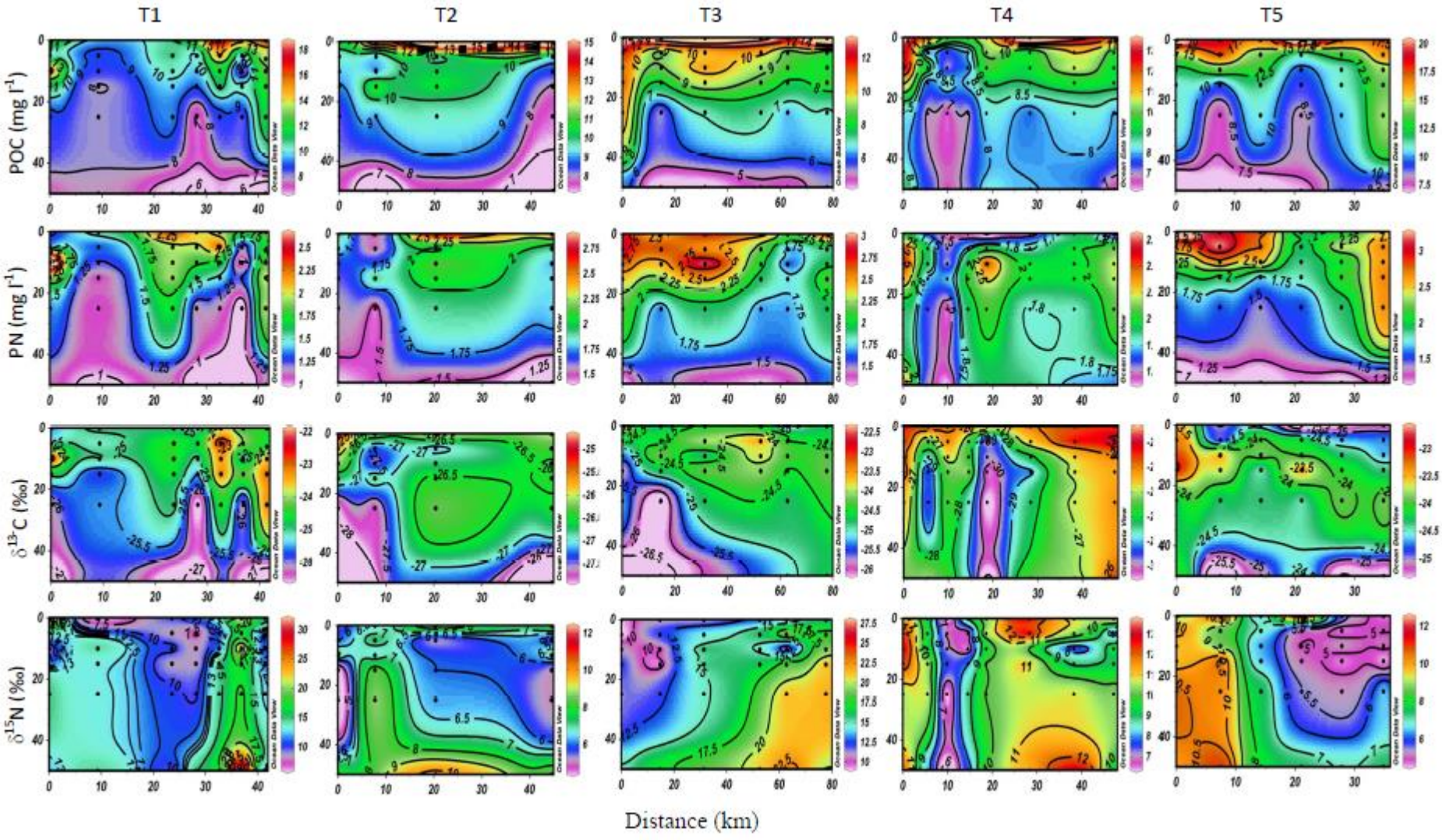

Fig. 3